Humanities & Social Sciences Communications

ARTICLE

https://doi.org/10.1057/s41599-025-05151-w OPEN

Monitoring changes in nighttime lights and anthropogenic CO_2 emissions during geopolitical conflicts from a remote sensing perspective

Zhenjie Liu[1]✉, Jun Li[1]✉, Haonan Chen[2]✉, Lizhe Wang[1]✉ & Antonio Plaza[3]✉

Monitoring spatiotemporal changes in anthropogenic CO_2 is crucial for informing international climate change policy initiatives, but also challenging due to the absence of national inventories and statistical data during such conflicts. Currently, nighttime light (NTL) remote sensing data is often used for spatial disaggregation of CO_2 emission statistics, while the construction of existing anthropogenic CO_2 emission datasets relies on ground observation data, which are difficult to apply rapidly and accurately in the context of a geopolitical conflict. This study introduces a novel model for monitoring monthly changes in anthropogenic CO_2 emissions based on NTL data collected by the Visible Infrared Imaging Radiometer Suite (VIIRS) and the Global Gridded Daily CO_2 Emission Dataset (GRACED). The proposed model integrates the monthly changes in NTL caused by the conflict with the monthly mean CO_2 emissions of various sectors before the conflict for near-real-time monitoring through spatial aggregation and statistical analysis using Google Earth Engine (GEE) and ArcGIS software. As a case study, we consider the Russia-Ukraine war to analyze the monthly CO_2 emission changes in Ukraine, across various scales. The results demonstrate that the residential consumption, ground transport, and industry sectors respectively have CO_2 emission changes of 413 kt, 106 kt, and 324 kt (six months after the war began), and of 136 kt, 33 kt, and 139 kt (one year after the war began) in Ukraine. Significant consistency between the estimated and reference CO_2 emission changes can be observed for each month during the war, with the R^2 ranging from 0.61–0.87, 0.51–0.74, and 0.69–0.93 for the residential consumption, ground transport, and industry sectors, respectively. Overall, this study contributes new insights into the monitoring of near-real-time changes in anthropogenic CO_2 emissions under geopolitical conflicts, and help to enhance the understanding of the environmental governance and climate accountability.

[1] School of Computer Science, China University of Geosciences, Wuhan, China. [2] Department of Electrical and Computer Engineering, Colorado State University, Fort Collins, USA. [3] Department of Technology of Computers and Communications, University of Extremadura, Cáceres, Spain.
✉email: liuzhenjie@cug.edu.cn; lijuncug@cug.edu.cn; haonan.chen@colostate.edu; lizhe.wang@foxmail.com; aplaza@unex.es

Introduction

Greenhouse gas emissions from human activities contribute to global warming (Guan et al. 2018; Han et al. 2024; Li et al. 2022). Greenhouse gases listed by the Kyoto Protocol include carbon dioxide (CO_2), methane (CH_4), nitrous oxide (N_2O), hydrofluorocarbons (HFCs), perfluorocarbons (PFCs), and sulfur hexafluoride (SF_6) (Telesetsky, 1999). CO_2 is an important indicator in global climate change simulation research and international climate policy (Valjarević et al. 2022). The natural carbon cycle maintains a relative balance in carbon revenue and expenditure, but human activities (such as burning fossil fuels and land use changes) increase CO_2 emissions, upsetting this equilibrium and influencing climate feedback mechanisms (Falkowski et al. 2000). According to measurements by the NOAA Global Monitoring Laboratory, CO_2 concentrations has risen from 336.85 ppm in 1979 to 422.77 ppm in 2024 (Lan et al. 2025). Nowadays, anthropogenic CO_2 is acknowledged as one of the primary sources of climate change (Hu et al. 2024; Rahman and Kashem, 2017). It is crucial to create national inventories to track anthropogenic CO_2 emissions in order to lessen the adverse effects of climate change (Shi et al. 2021). Under the Paris Agreement, Parties are required to determine and report their anthropogenic CO_2 emissions at the national level (Klein, 2017). Understanding the global carbon cycle and guaranteeing the effective execution of the United Nations Framework Convention on Climate Change (UNFCCC) depend on monitoring the spatiotemporal changes in anthropogenic CO_2 emissions (Hegglin et al. 2022; Li et al. 2022). This is also crucial for informing international climate change policy initiatives for sustainable development (Figueres et al. 2018; Hua et al. 2023).

National inventories focus on detailed information on CO_2 emissions from various human activities in peacetime (IPCC, 2006). In recent years, geopolitical conflicts have occurred frequently, and sociopolitical tensions have been rising in many parts of the world (Mortoja and Yigitcanlar, 2022; Söder, 2023). In this context, anthropogenic CO_2 and other greenhouse gas emissions are highly sensitive to abrupt disruptions in human activities. Geopolitical conflicts, for example, often result in the mass displacement of populations from urban and industrial centers, leading to substantial reductions or redistributions of emissions associated with residential activities and transportation (Gao et al. 2021). Simultaneously, conflicts inflict severe damage on power plants, industrial facilities, and fuel supply chains, causing profound disturbances in energy production and consumption patterns, which in turn significantly alter greenhouse gas emissions (Sasmoko et al. 2023). Nevertheless, monitoring and quantifying these emission changes remain a considerable challenge. Geopolitical conflicts often cause countries and regions to fall into political, economic, and social chaos, and government resources and attention are forced to turn to emergency and security affairs, thus weakening the ability to monitor and collect CO_2 emission data (Bun et al. 2023). In addition, during conflicts, infrastructure may be damaged, information transmission is interrupted or data management systems are paralyzed, resulting in the inability to determine and report anthropogenic CO_2 emissions (Bun et al. 2024). The lack of timely and reliable data makes it difficult to formulate and implement effective emission reduction strategies, posing serious challenges to fulfilling the emission reduction obligations under the Paris Agreement. Near-real-time monitoring techniques enable the timely detection of abnormal fluctuations in CO_2 and other greenhouse gas emissions during geopolitical conflicts, thereby providing robust data support for the periodic reporting obligations under the UNFCCC. Such datasets facilitate the quantitative assessment of emission variabilities during conflict periods, which is essential for ensuring the equitable allocation of carbon credits and the effective operation of compensation mechanisms within carbon trading schemes (Adediran and Swaray, 2023). Furthermore, these data lay the foundation for developing an accountability framework for conflict-related emissions (e.g., environmental damage compensation), thus informing decision-making processes for post-conflict carbon emission responsibility and advancing climate justice practices (Mubarik et al. 2024).

Global information on human activity can be visualized through Earth observations using nighttime light (NTL) satellites (Elvidge et al. 2009; Li and Cao, 2024; Zou et al. 2024). Common data sources include the Defense Meteorological Satellite Program Operational Linescan System (DMSP-OLS) (Huang et al. 2014) and the Suomi National Polar-Orbiting Partnership Visible Infrared Imaging Radiometer Suite (NPP-VIIRS) (Elvidge et al. 2017). On the one hand, NTL data have been considered as an effective tool for detecting geopolitical conflicts, such as the Iranian, Syrian, and Yemeni crises, among others (Jiang et al. 2017; Li et al. 2015, 2021). For example, the research in (Li and Li, 2014) revealed the national and provincial losses during the Syrian Civil War using monthly composites of data from DMSP-OLS. On the other hand, since NTL data can accurately depict the fine-grained spatial patterns of human activities, it has also been used to quantify anthropogenic CO_2 emissions at various administrative scales by spatially disaggregating statistical data (Gao et al. 2023; Guo and Wang, 2023). Some studies have put forward global CO_2 emission datasets by combining NTL data with ground observations (Gaughan et al. 2019). For instance, Oda and Maksyutov disaggregated national fuel estimates and created the Open Source Data Inventory for Anthropogenic CO_2 (ODIAC) using a point source database and NTL data (Oda et al. 2018). In a similar fashion, another widely used dataset that reports emissions as national totals and global gridmaps is the Emission Database for Global Atmospheric Research (EDGAR) (Crippa et al. 2020). There is typically a lag of more than a year or two in the generation of these datasets. Recently, the Global Gridded Daily CO_2 Emission Dataset (GRACED) was developed for near-real-time monitoring of anthropogenic CO_2 emissions by integrating several data streams, including point sources, national fossil fuel and cement, and country-level sectoral emissions (Dou et al. 2022; Liu et al. 2020a). Despite its ability to monitor changes in anthropogenic CO_2 emissions during geopolitical conflicts in a timely manner, GRACED is still constrained by the availability of statistical data and ground observations in conflict zones. Estimates of anthropogenic CO_2 emissions are obtained using data from other regions when relevant data in conflict zones is not available, which could lead to significant errors and uncertainty.

Based on the above research and potential deficiencies, this study integrates NTL data and GRACED to highlight spatiotemporal changes in anthropogenic CO_2 emissions during geopolitical conflicts. This study not only provides unique insights into how geopolitical conflicts rapidly change anthropogenic CO_2 emissions, but also helps to understand the broader environmental impacts of geopolitical conflicts. To achieve these goals, we choose Ukraine as the study domain, as it is experiencing drastic changes in anthropogenic CO_2 emissions during the Russia-Ukraine war. The main contributions of this work are summarized as follows: (1) The monthly changes in anthropogenic CO_2 of different sectors in Ukraine during the Russia-Ukraine war are estimated. (2) The spatial heterogeneity of the changes in anthropogenic CO_2 of different sectors in Ukraine during the Russia-Ukraine war is also analyzed.

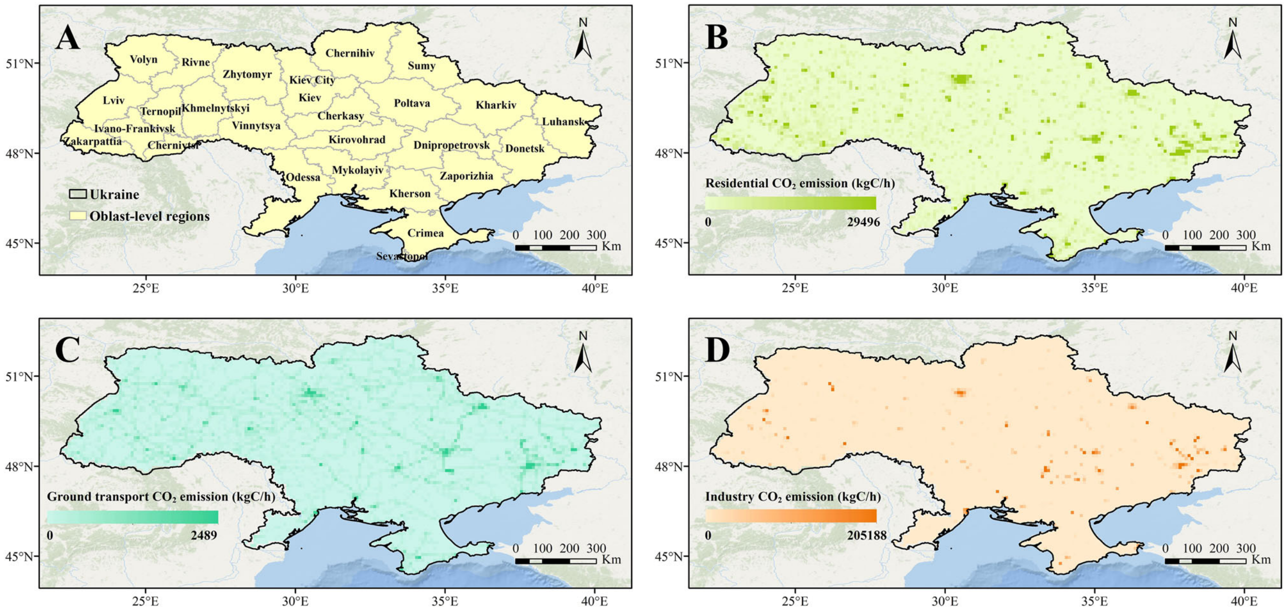

Fig. 1 Spatial distribution of sectoral CO_2 emissions. A Study domain and **B–D** CO_2 emissions of residential consumption, ground transport, and industry sectors across Ukraine in January 2022.

Materials and methods

This section introduces the study case, datasets, and our newly proposed model for monitoring changes in anthropogenic CO_2 emissions.

Study case. Since February 2022, Russia has invaded Ukraine on several fronts, with attacks on both military and civilian targets seriously affecting Ukraine's population displacement, national economy, and ecological environment (Rawtani et al. 2022). The impact of the Russia-Ukraine war goes far beyond the heavily industrialized area of fighting, as civilians in the hinterland and close to the front lines are constantly in danger from drone attacks, airstrikes, and indiscriminate shelling. The Armed Conflict Location & Event Data Project (ACLED) has recorded approximately 40,000 incidents of political violence in Ukraine, one year after the war began (Raleigh et al. 2010). Over 5 million Ukrainians have been internally displaced, and another 8 million have been compelled to apply for asylum outside. In this study, Ukraine (currently experiencing a Russian invasion) is chosen as a study domain to examine changes in anthropogenic CO_2 emissions (Fig. 1A).

Located in the East European Plain, Ukraine is the second largest country in Europe, with an area of approximately 603,500 square kilometers. The country presents a landscape consisting of fertile farmland, vast green areas, and highly urbanized and industrialized built-up areas (Fig. S1). Industrial activities are mainly concentrated in the regions of Donetsk, Luhansk, Dnipro, and Zaporizhia, while large green areas, including nature reserves, forests, meadows, and farmlands, serve as important buffers to mitigate urban heat islands and improve ecological services (Morar et al. 2022).

Ukraine experiences a temperate continental climate characterized by cold winters and warm summers, with pronounced temporal and spatial variability. Utilizing the Terra Moderate Resolution Imaging Spectroradiometer (MODIS) Land Surface Temperature/Emissivity Daily (MOD11A1) product, we derive the spatial distribution of average annual land surface temperatures in Ukraine for the years 2000, 2010, and 2020 (Fig. S2A–C), along with the temperature changes observed in 2020 relative to 2000 (Fig. S2D). Higher temperatures and significant warming trends are most evident in the southern and eastern regions, where industrial activities are heavily concentrated. These temperature shifts are closely linked to changes in vegetation phenology, extended growing seasons, and alterations in regional carbon cycles (Piao et al. 2007).

Data

VIIRS NTL imagery. A global daily measuring system for Earth system science and applications is provided by the Day-Night Band (DNB) sensor included in the VIIRS. The atmospheric and Lunar bidirectional reflectance (BRDF)-corrected Black Marble NTL product (VNP46A2) provides daily DNB data at 500 m spatial resolution, with operational correction for surface reflected lunar radiance (Román et al. 2018). We acquired daily NTL imagery over the study domain between January 1, 2021, and February 28, 2023, from the VNP46A2, which is publicly available from the National Centers for Environmental Information (NCEI) of the National Oceanic and Atmospheric Administration (NOAA). Then, we down-sample the collected NTL imagery to a spatial resolution of 10 km by grid summing.

GRACED. GRACED has been tracking the spatiotemporal fluctuation features of global anthropogenic CO_2 emissions from various sectors around the world since January 1, 2019, thus supporting adjustments of various climate policy measures. Specifically, GRACED is produced with a temporal resolution of one day and a global spatial resolution of 10 km. Here, we collect daily anthropogenic CO_2 emission data of residential consumption, ground transport, and industry sectors between January 1, 2021, and February 28, 2023, from GRACED. Figure 1B–D present the spatial distribution of anthropogenic CO_2 emissions from different sectors in Ukraine before the Russia-Ukraine war (i.e., January 2022).

Methods. Figure 2 presents a schematic overview of the proposed model for monitoring monthly changes in anthropogenic CO_2 emissions of different sectors using VIIRS NTL data and GRACED. We first aggregate the daily NTL data for each month during the war period using a minimum composite technique, and then calculate the monthly NTL changes relative to a

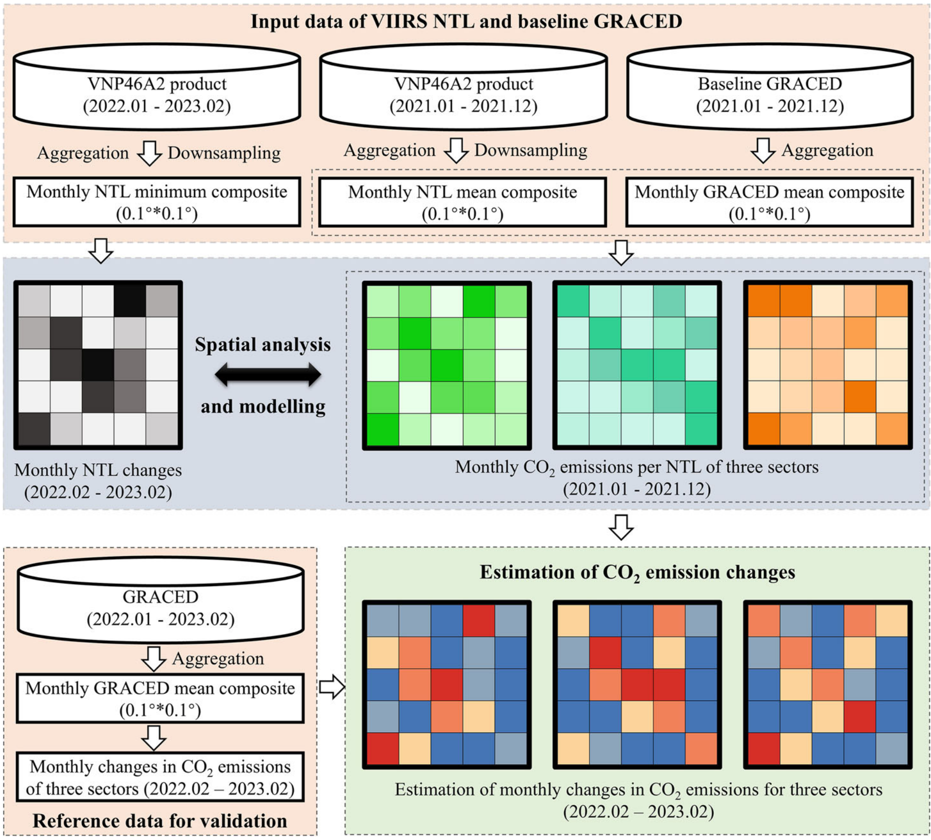

Fig. 2 Workflow for monitoring monthly changes in anthropogenic CO_2 emissions of different sectors using VIIRS NTL data and GRACED.

reference period. Meanwhile, the monthly mean composite NTL data and the monthly mean composite GRACED data from the year before the Russia-Ukraine war are used as baseline data for determining CO_2 emissions per unit of NTL. On this basis, the monthly changes in anthropogenic CO_2 emissions of different sectors during the war period are estimated and then validated by the monthly changes derived from the GRACED data during the war period and the reference period.

Monthly changes in the NTL composite. The monthly changes in NTL caused by the Russia-Ukraine war are reflected based on the difference between the NTL during the war period and the NTL during the reference period. Let $\mathrm{NTL}_{m_i,y_j} = \left\{\mathrm{NTL}^1_{m_i,y_j}, \ldots, \mathrm{NTL}^n_{m_i,y_j}\right\}$ be a set of daily NTL data, where n is the number of days for month i of year j. Given that NTL data are easily disturbed by abnormal factors such as fire and explosions during the war period (Ialongo et al. 2023; Wang et al. 2021), we generate the monthly minimum composite of NTL data (from January 2022 to February 2023) by using the minimum function of Google Earth Engine (GEE) to reduce data uncertainty as follows:

$$\mathrm{NTL}^{min}_{m_i,y_j} = \arg\min \mathrm{NTL}_{m_i,y_j}. \tag{1}$$

Then, the monthly minimum composite of NTL data is imported into the ArcGIS 10.7 software for spatial analysis. Taking January 2022 as a reference period before the war, the monthly changes in the NTL minimum composite during the war period are calculated using the raster calculator tool:

$$\mathrm{DNTL}_{m_i,y_j} = \mathrm{NTL}^{min}_{m_i,y_j} - \mathrm{NTL}^{min}_{Jan,2022}. \tag{2}$$

Considering the extensive destruction of civilian infrastructure and the resulting population relocation during the Russia-Ukraine war (Rawtani et al. 2022), we assume that the war period will not have a higher NTL value than the non-war period. As a result, these observations will not be included for subsequent estimation of the changes in CO_2 emissions when DNTL_{m_i,y_j} is larger than zero.

Estimation of monthly CO_2 emission changes. Here, we develop a spatial model to estimate the monthly changes in anthropogenic CO_2 emissions across several sectors. Based on the daily NTL data and daily anthropogenic CO_2 emission data from GRACED, the monthly mean composite NTL data and the monthly mean composite anthropogenic CO_2 emission data during the baseline period (from January 2021 to December 2021) are first generated via the mean function of GEE:

$$\mathrm{NTL}^{mean}_{m_i,y_j} = \arg\mathrm{mean}\,\mathrm{NTL}_{m_i,y_j}, \tag{3}$$

$$\mathrm{GRACED}^{mean}_{m_i,y_j,s_k} = \arg\mathrm{mean}\,\mathrm{GRACED}_{m_i,y_j,s_k}, \tag{4}$$

$\mathrm{GRACED}_{m_i,y_j} = \left\{\mathrm{GRACED}^1_{m_i,y_j,s_k}, \ldots, \mathrm{GRACED}^n_{m_i,y_j,s_k}\right\}$ is a set of daily GRACED data of sector k, and n is the number of days for month i of year j (i.e., 2021).

Then, the monthly mean composite is imported into the ArcGIS 10.7 software. The subsequent formulas are all numerically calculated using the raster calculator tool of the software. The monthly CO_2 emissions per unit of NTL of different sectors during the baseline period are calculated by:

$$\mathrm{CEPN}_{m_i,y_j,s_k} = \frac{\mathrm{GRACED}^{mean}_{m_i,y_j,s_k}}{\mathrm{NTL}^{mean}_{m_i,y_j}}. \tag{5}$$

Based on the monthly changes in the NTL minimum composite during the war period (Eq. (2)) and the monthly

CO_2 emissions per unit of NTL during the baseline period (Eq. (5)), we estimate the monthly changes in anthropogenic CO_2 emissions of different sectors. Specifically, the monthly changes in CO_2 emissions in the residential consumption sector (relative to the reference period) are estimated as follows:

$$\mathrm{MCCE}_{m_i,y_j,residential} = \mathrm{TAF}_{m_i} \times \mathrm{CEPN}_{m_i,y_j,residential} \times \mathrm{DNTL}_{m_i,y_j}, \quad (6)$$

where TAF_{m_i} is a temperature adjustment factor for compensating the variations in air temperature that are considered in GRACED. The TAF_{m_i} is calculated according to the monthly mean composite of GRACED data during the baseline period:

$$\mathrm{TAF}_{m_i} = \frac{\mathrm{GRACED}^{mean}_{m_i,2021}}{\mathrm{GRACED}^{mean}_{Jan,2021}}. \quad (7)$$

Given that the frequent movement, displacement, and humanitarian assistance of Ukrainian civilians during the war will lead to intensive transport activities and CO_2 emissions, the monthly changes in CO_2 emissions ofthe ground transport sector relative to the reference period are estimated as follows:

$$\mathrm{MCCE}_{m_i,y_j,transport} = (-1) \times \mathrm{CEPN}_{m_i,y_j,transport} \times \mathrm{DNTL}_{m_i,y_j}. \quad (8)$$

Concerning the industry sector, the monthly changes in CO_2 emissions relative to the reference period are estimated by multiplying the monthly changes in the NTL minimum composite during the war period and the monthly CO_2 emissions per unit of NTL during the baseline period:

$$\mathrm{MCCE}_{m_i,y_j,industry} = \mathrm{CEPN}_{m_i,y_j,industry} \times \mathrm{DNTL}_{m_i,y_j}. \quad (9)$$

Note that the geographic coordinate system of all the input and output data mentioned above is the World Geodetic System 1984 (WGS84). The spatial distribution of resultant CO_2 emissions across different sectors is extracted according to the extent of Ukraine using the clip tool of ArcGIS 10.7 software and exported.

Validation of monthly CO_2 emission changes. Here, we generate monthly mean composites of GRACED data by aggregating the daily GRACED data (Eq. (4)) during the war period (from February 2022 to February 2023) and the reference period (i.e., January 2022). Then, the monthly changes in the GRACED mean composite of different sectors relative to the reference period are calculated by:

$$\mathrm{DGRACED}_{m_i,y_j,s_k} = \mathrm{GRACED}^{mean}_{m_i,y_j,s_k} - \mathrm{GRACED}^{mean}_{Jan,2022,s_k}. \quad (10)$$

$\mathrm{DGRACED}_{m_i,y_j,s_k}$ is used as the ground truth for validating the monthly CO_2 emission changes estimated from VIIRS NTL data. In particular, we use linear regression to compare the estimated and ground truth values. According to the R^2 and slope fitting metrics, we examine the effectiveness of the proposed spatial model for estimating monthly changes in CO_2 emissions of different sectors.

Results

In this section, we first analyze the NTL changes in Ukraine across various scales. Then, the estimation of changes in CO_2 emissions of different sectors is performed.

NTL changes in Ukraine across various scales. Figure 3 A–C present the monthly NTL minimum composite in January 2022 (one month before the war began), August 2022 (six months after the war began), and February 2023 (one year after the war began). With the war going on, Ukraine has suffered a precipitous decrease in NTL, with many illuminated areas becoming dark. For quantitative analysis, we first assess NTL changes at the oblast (administrative division or region) scale (Fig. 3D). Compared with the western region in the hinterland, the central and eastern regions close to the front lines exhibit relatively more NTL reduction. Six months on from the invasion, 63% of oblasts show a reduction of more than 50% in NTL. One year on from the invasion, the NTL in oblasts of Lviv, Kiev, Poltava, Dnipropetrovsk, and Kharkiv decreased by 41%, 78%, 67%, 75%, and 69%, respectively.

In addition, we select seven cities severely affected by the war for further analysis, including Lviv City, Kiev City, Kherson City, Dnipropetrovsk City, Zaporizhia City, Kharkiv City, and Donetsk City (Fig. 3E). The NTL in the cities of Kiev, Dnipropetrovsk, Zaporizhia, and Kharkiv has a reduction of more than 60% six months after the war began. And the cities of Kiev, Kherson, Dnipropetrovsk, Zaporizhia, and Kharkiv show a reduction in NTL of more than 80% one year after the war began. In contrast, while being threatened and attacked by drone attacks and airstrikes, Lviv City in eastern Ukraine exhibits a relatively lower drop in NTL. It can also be found that the NTL of Donetsk City has not changed significantly. On the one hand, this may be due to the fact that this city has been in conflict since 2014, resulting in a small difference between the NTL during the war and during the reference period. On the other hand, as the main conflict area between Russia and Ukraine, the frequent explosions and flames in Donetsk City may also lead to abnormalities and uncertainty in the NTL.

Estimation of changes in CO_2 emissions of different sectors. Based on the aforementioned NTL changes in Ukraine, we estimate the changes in CO_2 emissions of residential consumption, ground transport, and industry sectors, respectively (Figs. 4–6). The spatial distribution of residential consumption CO_2 emission declines in Ukraine is presented in the Fig. 4A and D. Relative to the reference period, a total of 413 kt and 136 kt declines in residential consumption CO_2 emissions are observed six months and one year after the war began, respectively. The CO_2 emissions in the residential consumption sector are counted at the oblast scale (Fig. 4C and F). Six months after the war began, the top five oblasts with the largest decline in monthly CO_2 emissions are Kiev (59 kt), Dnipropetrovsk (47 kt), Kharkiv (43 kt), Lviv (33 kt), and Donetsk (32 kt). One year after the war began, the top five oblasts with the largest decline in monthly CO_2 emissions are Kiev (19 kt), Kharkiv (17 kt), Dnipropetrovsk (14 kt), Donetsk (14 kt), and Odessa (7 kt). As for the ground transport sector, the spatial distribution of CO_2 emission increases in Ukraine is presented in Fig. 5A and D. In total, 106 kt and 33 kt increases in ground transport CO_2 emissions are observed six months and one year after the war began, respectively. Figure 5C and F present the oblast-scale CO_2 emissions of the ground transport sector. Six months after the war began, the top five oblasts with the largest decline in monthly CO_2 emissions are Dnipropetrovsk (13 kt), Kiev (11 kt), Kharkiv (9 kt), Donetsk (8 kt), and Lviv (6 kt). One year after the war began, the top five oblasts with the largest decline in monthly CO_2 emissions are Dnipropetrovsk (5 kt), Donetsk (4 kt), Kharkiv (4 kt), Kiev (4 kt), and Poltava (2 kt). Regarding the industry sector, the spatial distribution of CO_2 emission declines in Ukraine is presented in Fig. 6A and D. Six months and one year after the war began, 324 kt and 139 kt declines in ground transport CO_2 emissions are observed, respectively. Figure 6C and F present the oblast-scale CO_2 emissions of industry sector. Six months after the war began, the top five oblasts with the largest decline in monthly CO_2 emissions are Dnipropetrovsk (126 kt), Zaporizhia (47 kt), Donetsk (22 kt),

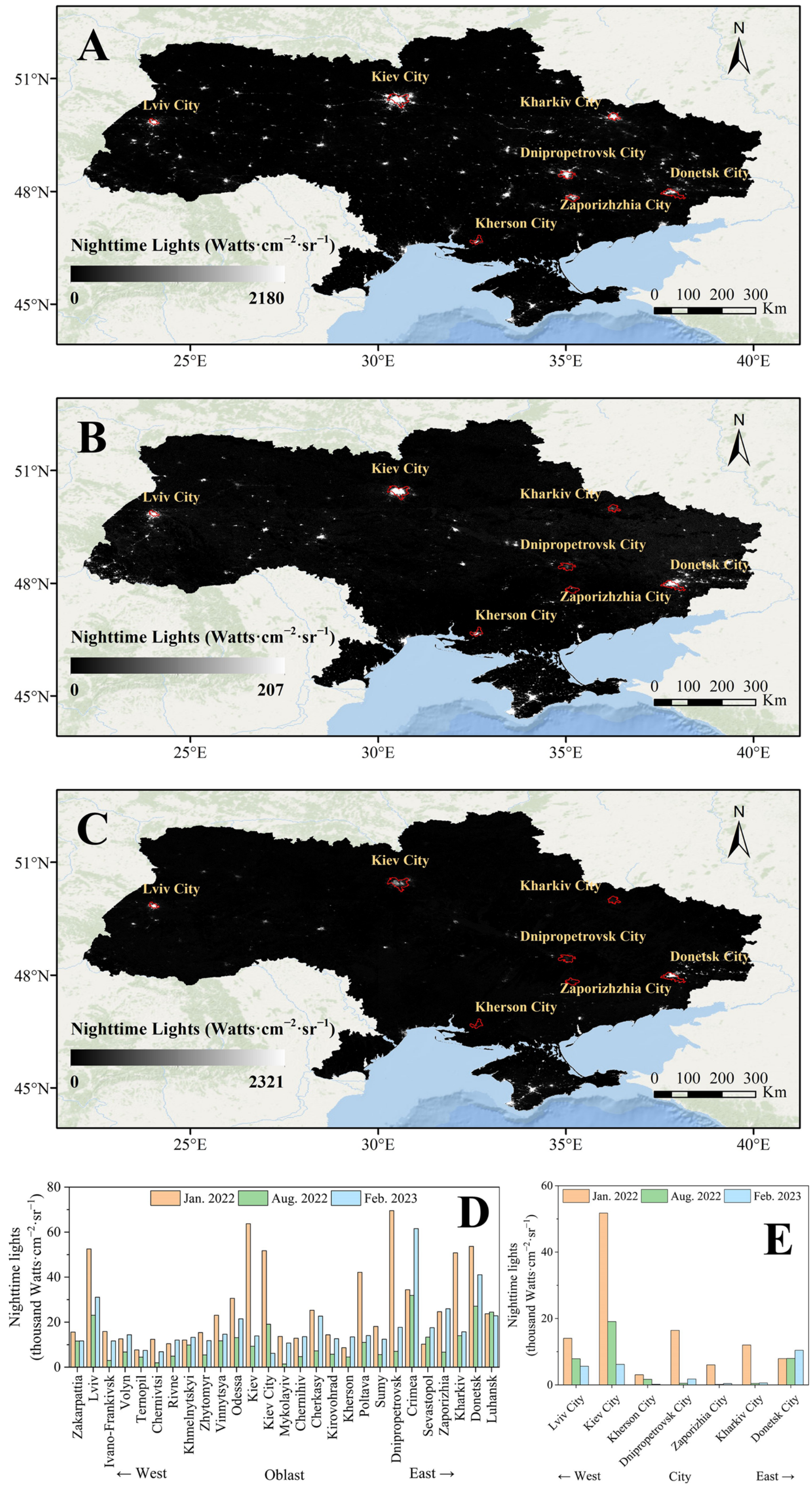

Fig. 3 Monthly NTL minimum composite and changes. Monthly NTL minimum composite in Ukraine in **A** January 2022, **B** August 2022, and **C** February 2023, and NTL changes at **D** oblast scale and **E** city scale.

Lviv (17 kt), and Luhansk (12 kt). One year after the war began, the top five oblasts with the largest decline in monthly CO_2 emissions are Dnipropetrovsk (57 kt), Zaporizhia (24 kt), Donetsk (13 kt), Luhansk (12 kt), and Kharkiv (5 kt).

Linear regression analyses are conducted to assess the degree of agreement between the estimated and reference CO_2 emissions for each sector throughout the war period. For the residential consumption sector, there is a significant degree of congruence

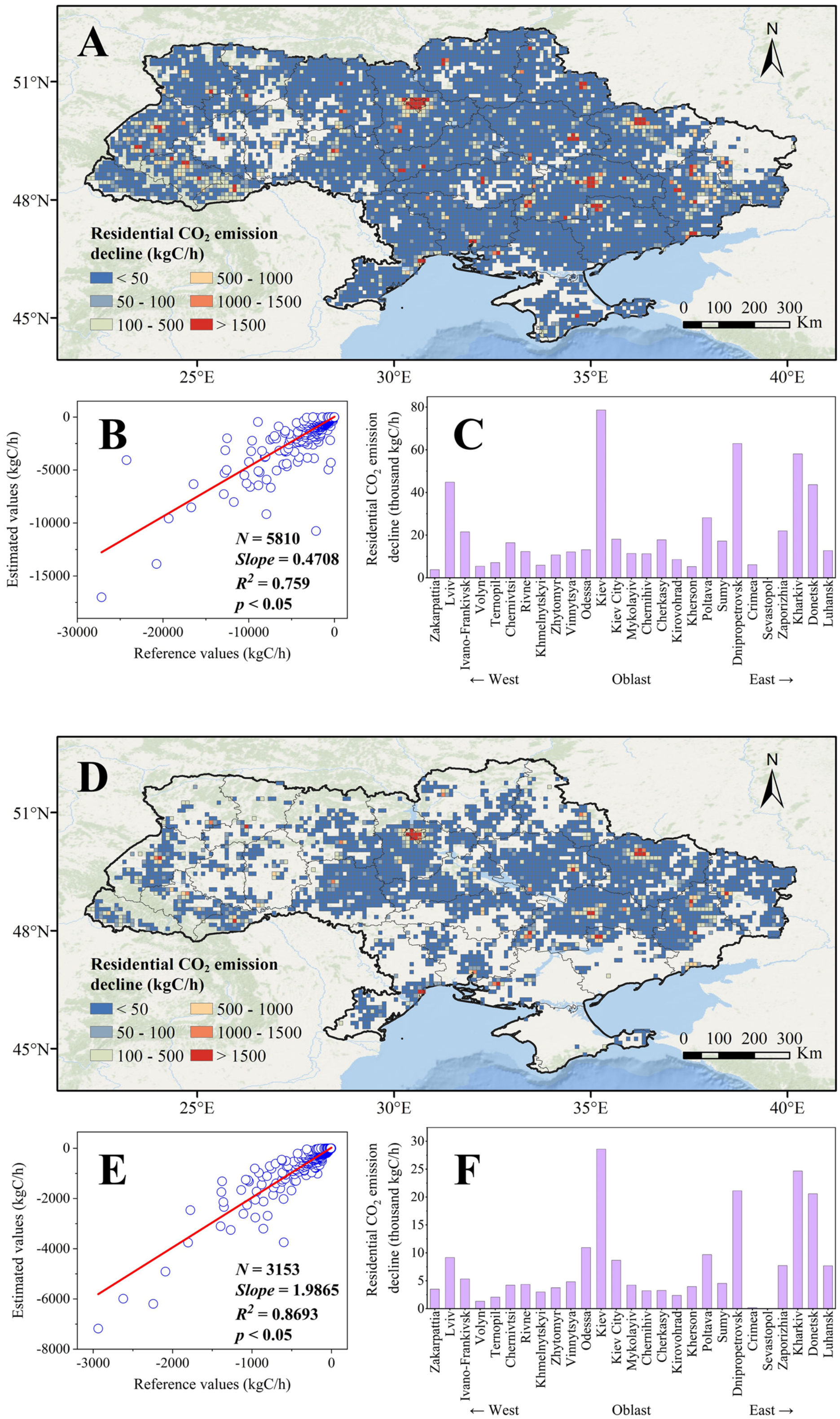

Fig. 4 Residential consumption CO_2 emission changes. **A** National spatial distribution, **B** linear regression, and **C** oblast-level estimation of residential consumption CO_2 emission decline six months after the invasion. **D** National spatial distribution, **E** linear regression, and **F** oblast-level estimation of residential consumption CO_2 emission decline one year after the invasion.

between the estimated and reference values in both August 2022 ($R^2 = 0.76$, $\rho < 0.05$) and February 2023 ($R^2 = 0.87$, $\rho < 0.05$) (Fig. 4B and E). For the ground transport sector, the estimated and reference values exhibit a substantial degree of consistency in both August 2022 ($R^2 = 0.64$, $\rho < 0.05$) and February 2023 ($R^2 = 0.74$, $\rho < 0.05$) (Fig. 5B and E). For the industry sector, linear regression results demonstrate significant consistency between the estimated and reference values in both August 2022 ($R^2 = 0.91$, ρ

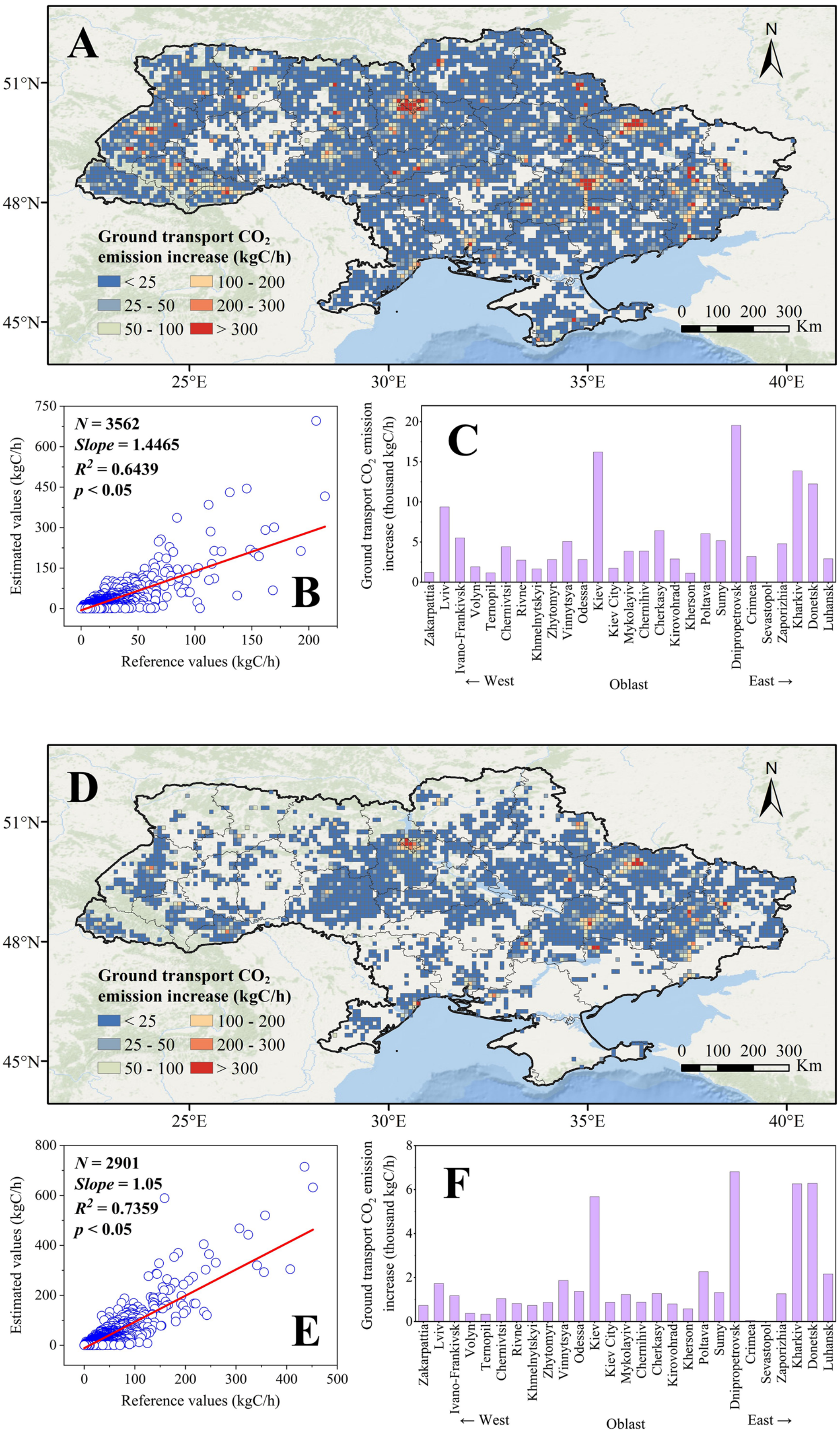

Fig. 5 Ground transport CO_2 emission changes. **A** National spatial distribution, **B** linear regression, and **C** oblast-level estimation of ground transport CO_2 emission decline six months after the invasion. **D** National spatial distribution, **E** linear regression, and **F** oblast-level estimation of ground transport CO_2 emission decline one year after the invasion.

< 0.05) and February 2023 ($R^2 = 0.89$, $\rho < 0.05$) (Fig. 6B and E). Additionally, Tables S1–S3 provide the statistical findings of linear regression on the monthly variations in the estimated and reference CO_2 emissions of different sectors. There is a notable degree of agreement between the estimated and reference values for each month during the war. Specifically, the R^2 ranges from 0.61-0.87, 0.51-0.74, and 0.69-0.93 for the residential consumption, ground transport, and industry sectors, respectively.

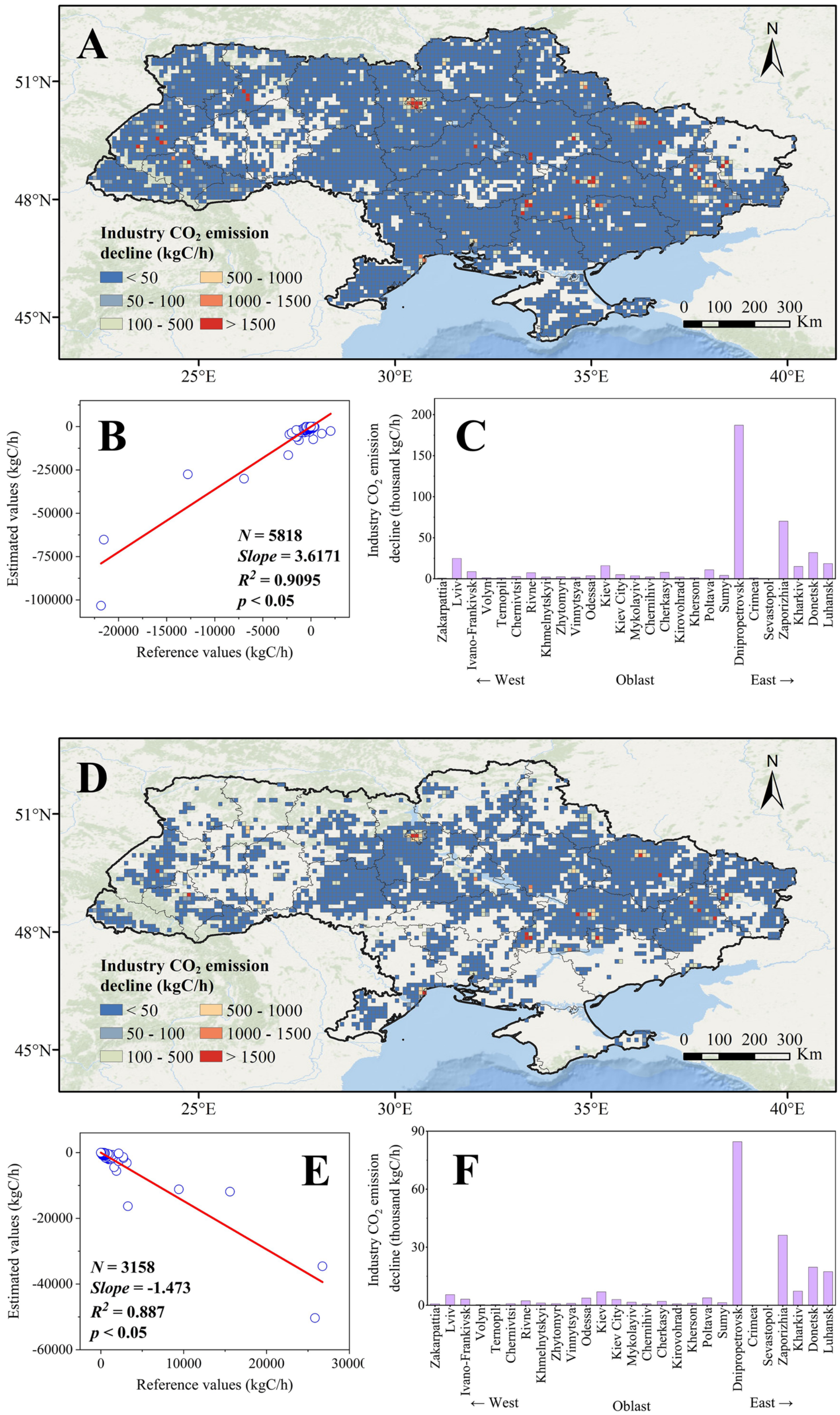

Fig. 6 Industry CO_2 emission changes. **A** National spatial distribution, **B** linear regression, and **C** oblast-level estimation of industry CO_2 emission decline six months after the invasion. **D** National spatial distribution, **E** linear regression, and **F** oblast-level estimation of industry CO_2 emission decline one year after the invasion.

Furthermore, the monthly changes in CO_2 emissions of different sectors relative to the reference period are shown for the whole Ukraine and also for seven cities severely affected by the war, i.e., Dnipropetrovsk City, Donetsk City, Zaporizhzhia City, Kiev City, Kharkiv City, Kherson City, and Lviv City (Fig. 7). Since the invasion in late February 2022, the ongoing war in the first half of the year has caused significant changes in CO_2 emissions of different sectors relative to January 2022.

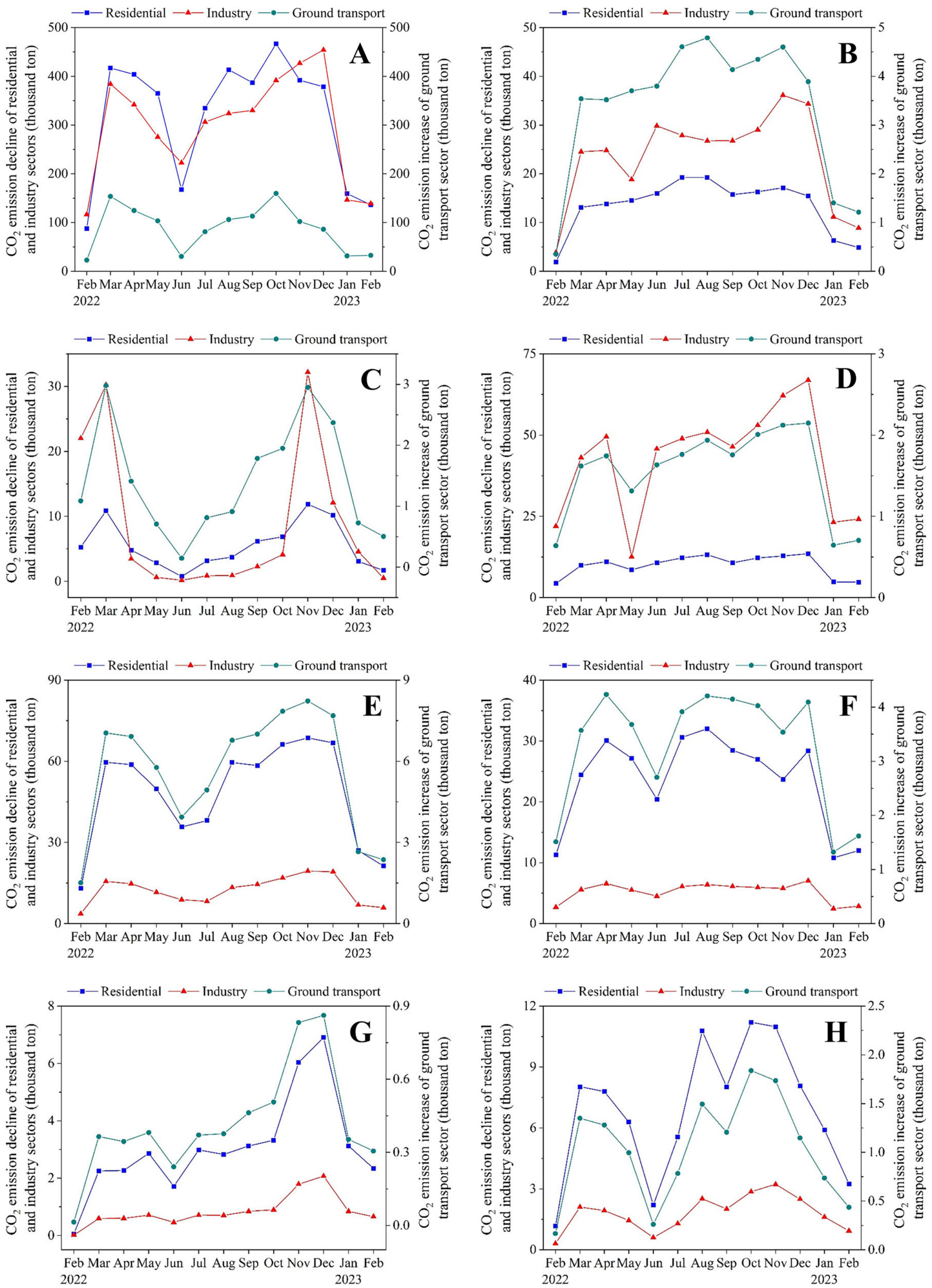

Fig. 7 Monthly sectoral CO_2 emission trends. Monthly changes in CO_2 emissions of different sectors for **A** the whole Ukraine, **B** Dnipropetrovsk City, **C** Donetsk City, **D** Zaporizhzhia City, **E** Kiev City, **F** Kharkiv City, **G** Kherson City, and **H** Lviv City.

Beginning in mid-September, the Russia-Ukraine war was reduced from a full-scale war to a local war due to the declaration of defeat on Russia's fronts in the Kiev and Kharkov directions. Then, Russia began regular air and missile attacks on Ukraine's energy facilities and civilian infrastructure from October to December 2022, resulting in more pronounced changes in CO_2 emissions of different sectors during this period.

Discussion

In the context of Russia-Ukraine war, this research estimates the monthly changes in CO_2 emissions of different sectors using NTL imagery. The spatial heterogeneity of the anthropogenic CO_2 changes is also uncovered across various scales. According to the results of linear regression tests, the estimated changes exhibit good consistency with the reference changes from the GRACED data during the war (Tables S1–S3). However, the difference between the estimated and reference values of different sectors needs to be investigated. Regarding the residential consumption sector, GRACED calculated CO_2 emissions by assuming that the annual totals remain unchanged (Dou et al. 2022; Liu et al. 2020a). The war-induced changes in residential consumption CO_2 emissions from the GRACED data could be ignored or underestimated. The estimated changes derived from NTL data are greater than those derived from GRACED, and the slopes of linear regression are larger than 1. As for the ground transport sector, GRACED calculated CO_2 emissions by makingthe assumption that there would be little change in the spatial distribution of ground transport within a nation (Dou et al. 2022; Liu et al. 2020a). But the massive population movement and displacement at the beginning of the war, as well as the return of civilians and the regularization of air and missile attacks after September 2022, are likely to exacerbate CO_2 emissions related to ground transport. Correspondingly, the estimated values are larger than the reference values in those months, with the slopes of linear regression being larger than one. Concerning the industry sector, the slopes of linear regression are not consistently positive or negative. It may be explained by the fact that statistical information on industrial production and electrical generation in Ukraine during the conflict was unavailable (Dou et al. 2022; Liu et al. 2020a). In this case, datasets from other countries or regions are adopted for calculating industry CO_2 emissions in GRACED. Therefore, it is reasonable that the estimated changes in industry CO_2 emissions are much larger than the reference changes from GRACED. In addition, it can be observed from the results in Tables S4 that the fitting effects of the three sectors are different. The fitting results of residential consumption and industry sectors are better than those of the ground transport sector, which could be related to the difference in activity intensity reflected by NTL in various sectors and NTL sensor limitations. On the one hand, various human activities produce different lighting intensities and durations at night, which determines the different abilities of light data to capture changes in these activities (Shi et al. 2021). The industry and residential consumption sectors usually produce consistent and stable NTL signals, while the activities of the ground transport sector are mainly manifested in road lighting and moving vehicle lights, which are more dispersed in space and highly time-varying, making it difficult to stably reflect their overall activity level through a single indicator. On the other hand, NTL data have issues with sensor saturation or insufficient resolution in different brightness ranges (Sun et al. 2024; Zheng et al. 2023). NTL in concentrated industrial and residential areas is relatively less susceptible, while scattered and weaker road and vehicle lights are more susceptible to sensor limitations and atmospheric interference, which could statistically increase data uncertainty and regression model errors.

To further highlight the contribution and methodological advantages of this study, the following discussion will focus on three aspects by comparing with related research: overcoming the limitations of conventional carbon satellites in detecting weak changes in anthropogenic CO_2 emissions, resolving the issue of ground data scarcity during geopolitical conflicts, and offering data support for climate accountability and policy making. So far, many existing studies have demonstrated the effectiveness of using carbon satellites to monitor atmospheric CO_2 concentrations (Pan et al. 2021; Wang et al. 2024; Wilmot et al. 2024). But in reality, changes in anthropogenic CO2 emissions are typically far less significant than variations in concentrations caused by transportation and interannual variability in the atmosphere (Liu et al. 2023a). It is challenging to precisely record such small changes using carbon satellite data. By combining global CO_2 emission datasets prior to the conflict (e.g., GRACED) with NTL data during the conflict, this study offers a novel model to monitor changes in anthropogenic CO_2 emissions in the context of geopolitical conflicts. To a certain degree, the proposed model could compensate for the limitations of carbon satellite data. In addition, the current global CO_2 emissions datasets can well reflect the spatiotemporal characteristics of CO_2 emissions from different human activities (Crippa et al. 2020; Dou et al. 2022; Oda et al. 2018). However, the statistical reports and ground observation data for dataset construction are often difficult to obtain or updated with lags during geopolitical conflicts (Levin et al. 2018; Ratnayake et al. 2022). This study uses NTL data as an alternative indicator, which not only compensates for the lack of data but also captures the immediate impact of conflict on CO_2 emissions by comparing pre-war data with near-real-time changes. Furthermore, some studies have made significant progress in the development of policy frameworks and the adjustment of policy measures in recent years, such as the carbon market mechanism (Asadnabizadeh and Moe, 2024; Redmond and Convery, 2015; Schneider and La Hoz Theuer, 2019) and the climate accountability framework (Atapattu, 2020; Mees and Driessen, 2019; Williams, 2020). And policy design is gradually shifting towards data-driven, transparent, and cross-departmental coordination (Ali and Kamraju, 2025; van Deursen and Gupta, 2024; Hughes et al. 2020). However, it is challenging to satisfy the timely and reliable emission data demands of international regulators and policymakers, particularly in unpredictable contexts like geopolitical conflicts, because of inadequate measurement precision or a lack of frequent data updates (Ali and Thakkar, 2023; Feng et al. 2024). At the policy level, the proposed model can support spatial data on CO_2 emissions in a dynamic manner. This will help improve the implementation of the climate accountability framework, in addition to providing decision makers with a new tool to assess CO_2 emission changes in the context of conflict.

In the following, the limitations of this research and corresponding potential future research lines are discussed. First of all, Despite NTL imagery demonstrates great potential for anthropogenic CO_2 monitoring during geopolitical conflicts, numerous research has demonstrated that the accuracy of NTL for CO_2 emission estimation depends on a number of variables, including the population, economy, and natural environment (Liu et al. 2018; Shi et al. 2019; Sun et al. 2024). In particular, NTL tends to exhibit higher uncertainty for less developed or rural areas of the world with poor lighting (Pandey et al. 2017). In order to overcome such limitations (and the lack of NTL data) for anthropogenic CO_2 emission estimation under geopolitical conflicts, it is of great importance to introduce point source data to enhance the understanding of spatiotemporal relationships between NTL and CO_2 emissions. Specifically, social media data and data on political violence events can be considered (Liu et al. 2020b, 2024b; Raleigh et al. 2010). For example, some studies have modeled population displacements in Ukraine during the Russia-Ukraine war using social media data from sources including Facebook's advertising platform and Twitter (Leasure et al. 2023; Liu et al. 2024). The near real-time data on the ongoing geopolitical conflicts from ACLED also provides spatial information on different types of political violence events that can also be used to reveal conflict-related CO_2 emission processes and their environmental impact, including the use of petroleum products in military activities, the decomposition of war waste and fires in infrastructure, forests, and petroleum storage depots (Bun et al. 2024; Rawtani et al. 2022). Second, the current models may have oversimplified assumptions in complex and dynamically changing situations, and may not be able to fully eliminate the impact of factors such as temporary controls and damaged infrastructure. In future research, machine learning and deep learning can be introduced into the current model to capture nonlinear relationships and the impact of sudden events, thereby improving the model's prediction accuracy and robustness for CO_2 emission changes in complex environments (Ali et al. 2025; Bianchi and Putro, 2024; Guth and Sapsis, 2019; Qi and Majda, 2020). Third, this study is limited to analyzing the spatiotemporal changes in CO_2 emissions under geopolitical conflict scenarios. A key direction for future research is to migrate the model to other emergency scenarios on a global scale, such as natural disasters (Mu et al. 2024), public health crises (Lan et al. 2021), energy crises (Liu et al. 2023), and others. In these different scenarios, energy consumption and human activity patterns may change significantly, which in turn affects the dynamics of CO_2 emissions (Anser, 2019; Liu et al. 2022; Yu et al. 2022). By comparing cross-domain applications and verifications, the universality of the current model can be further validated. On this basis, a unified and flexible framework can be constructed to provide data support and a more comprehensive scientific basis for global climate accountability and environmental governance.

Conclusion

We develop a new spatial model based on VIIRS NTL and GRACED data to monitor monthly changes in anthropogenic CO_2 emissions of different sectors during geopolitical conflicts. Taking the Russia-Ukraine war as a case study, we estimate the monthly changes in CO_2 emissions of different sectors and reveal the spatial heterogeneity of CO_2 emission changes across various scales. Relative to January 2022, residential consumption, ground transport, and industry sectors are respectively observed to have CO_2 emission changes of 413 kt, 106 kt, and 324 kt (six months after the war began), and of 136 kt, 33 kt, and 139 kt (one year after the war began). There is significant consistency between the estimated and reference CO_2 emission changes for each month during the war. The R^2 ranges from 0.61-0.87, 0.51-0.74, and 0.69-0.93 for the residential consumption, ground transport, and industry sector, respectively. In conclusion, this study provides a new perspective to improve the understanding of CO_2 emission changes under geopolitical conflicts, as well as the potential use of applying the proposed spatial model to ongoing geopolitical conflicts around the world. Future perspectives include not only deepening the technical level of existing methods, but also expanding to multi-modal data fusion and interdisciplinary collaborative research, so as to build a more flexible and efficient system for global environmental monitoring and CO_2 emission management. Specifically, the integration of multi-source remote sensing data and ground monitoring data can be explored to improve the spatiotemporal resolution of CO_2 emission monitoring in geopolitical conflicts and emergency situations. In addition, advanced technologies such as machine learning and deep learning can be considered to further optimize data correction and model prediction capabilities, so as to provide more accurate and real-time data support for policy making, climate accountability, and environmental emergency management.

Policy recommendations. This study reveals the spatiotemporal impact of geopolitical conflicts on anthropogenic CO_2 emissions from a remote sensing perspective. Relevant policies should make full use of this technology and data advantages to optimize the environmental monitoring system and enhance CO_2 emission management capabilities. First, it is recommended that governments and international organizations increase investment to build a monitoring system that integrates multiple remote sensing data, such as nighttime lights, thermal infrared, aerosols, and high-resolution optical images. This system can not only complement the advantages of different data and improve the accuracy of capturing emission changes, but also achieve all-weather and dynamic monitoring (Jiang et al. 2023; Tian et al. 2024). Meanwhile, the system should have automated data processing and real-time early warning functions to ensure that abnormal fluctuations in environmental indicators can be quickly reflected in emergency situations, providing a scientific basis for government decision-making and emergency response.

Second, geopolitical conflicts and emergencies often go beyond the jurisdiction of a single country or department. Therefore, monitoring and assessing CO_2 emission change requires cross-departmental and cross-regional collaboration (Xu et al. 2025). It is recommended that governments, scientific research institutions, international organizations and private enterprises build data sharing and joint monitoring mechanisms, break down information silos and establish a multilateral cooperation framework. By regularly holding international seminars and joint experimental projects, all parties can discuss issues such as data integration, model improvement, and emergency plans, thereby improving the accuracy and credibility of monitoring results.

Third, environmental governance and climate policy formulation cannot be separated from public supervision and extensive participation. It is recommended to build an open and transparent environmental data sharing platform to regularly release remote sensing monitoring data, emission estimation results and related analysis reports to the public. Transparent information disclosure will not only help to improve the accountability of governments and enterprises in carbon emission reduction, but also create conditions for public participation in environmental decision-making (Hahn et al. 2015; Li et al. 2017). This will help promote the formation of a green development model with the participation of the whole society and provide real and timely data information support for the international climate accountability framework.

Data availability

The VIIRS NTL data are available at https://ladsweb.modaps.eosdis.nasa.gov. The CO_2 emissions data of GRACED are available at https://www.carbonmonitor-graced.com.

Received: 16 January 2025; Accepted: 29 May 2025;
Published online: 04 July 2025

References

Adediran IA, Swaray R (2023) Carbon trading amidst global uncertainty: The role of policy and geopolitical uncertainty. Econ Model 123:106279

Ali AH, Thakkar R (2023) Climate changes through data science: understanding and mitigating environmental crisis. Mesopotamian J Big Data 2023:125–137

Ali MA, Kamraju M (2025) Accountability, transparency, and adaptation strategies. In: Global Climate Governance: Strategies for Effective Management. Springer, p 135–154

Ali MI, Rahaman MA, Ali MJ (2025) The growth–environment nexus amid geopolitical risks: cointegration and machine learning algorithm approaches. Discov Sustain 6:1–24

Anser MK (2019) Impact of energy consumption and human activities on carbon emissions in Pakistan: application of stirpat model. Environ Sci Pollut Res 26:13453–13463

Asadnabizadeh M, Moe E (2024) A review of global carbon markets from Kyoto to Paris and beyond: The persistent failure of implementation. Front Environ Sci 12:1368105

Atapattu S (2020) Climate change and displacement: protecting 'climate refugees' within a framework of justice and human rights. J Hum Rights Environ 11:86–113
Bianchi O, Putro HP (2024) Artificial intelligence in environmental monitoring: Predicting and managing climate change impacts. Int Trans Artif Intell 3:85–96
Bun R, Marland G, Oda T et al. (2023) Estimating greenhouse gas emissions in a politically unstable world: A war in Ukraine and new challenges for emissions monitoring. SSRN Electron J
Bun R, Marland G, Oda T (2024) Tracking unaccounted greenhouse gas emissions due to the war in Ukraine since 2022. Sci Total Environ 914:169879
Crippa M, Guizzardi D, Muntean M et al. (2020) Fossil CO2 emissions of all world countries. Publications Office of the European Union, Luxembourg
van Deursen M, Gupta A (2024) Transparency is what states make of it: whose climate priorities are reflected in the Paris agreement's enhanced transparency framework? Clim Policy 24:1293–1308
Dou X, Wang Y, Ciais P et al. (2022) Near-real-time global gridded daily co2 emissions. The Innovation 3(1)
Elvidge CD, Sutton PC, Tuttle, BT et al. (2009) Global urban mapping based on nighttime lights. In: Global mapping of human settlement. CRC Press, p 157–172
Elvidge CD, Baugh K, Zhizhin M (2017) VIIRS night-time lights. Int J Remote Sens 38:5860–5879
Falkowski P, Scholes RJ, Boyle E (2000) The global carbon cycle: a test of our knowledge of Earth as a system. Science 290:291–296
Feng Y, Pan Y, Lu S (2024) Identifying the multiple nexus between geopolitical risk, energy resilience, and carbon emissions: evidence from global data. Technol Forecast Soc Chang 208:123661
Figueres C, Le Quéré C, Mahindra A et al. (2018) Emissions are still rising: ramp up the cuts
Gao C, Tao S, He Y (2021) Effect of population migration on spatial carbon emission transfers in China. Energy Policy 156:112450
Gao F, Wu J, Xiao J (2023) Spatially explicit carbon emissions by remote sensing and social sensing. Environ Res 221:115257
Gaughan AE, Oda T, Sorichetta A (2019) Evaluating nighttime lights and population distribution as proxies for mapping anthropogenic CO_2 emission in Vietnam, Cambodia and Laos. Environ Res Commun 1:091006
Guan D, Meng J, Reiner DM (2018) Structural decline in China's CO_2 emissions through transitions in industry and energy systems. Nat Geosci 11:551–555
Guo J, Wang H (2023) Study on carbon emission reduction effect of institutional openness in china. Sci Rep 13:254
Guth S, Sapsis TP (2019) Machine learning predictors of extreme events occurring in complex dynamical systems. Entropy 21:925
Hahn R, Reimsbach D, Schiemann F (2015) Organizations, climate change, and transparency: Reviewing the literature on carbon disclosure. Organ Environ 28:80–102
Han H, Zeeshan Z, Talpur BA (2024) Studying long-term relationship between carbon emissions, soil, and climate change: Insights from a global earth modeling framework. Int J Appl Earth Obs Geoinf 130:103902
Hegglin MI, Bastos A, Bovensmann H (2022) Space-based Earth observation in support of the UNFCCC Paris agreement. Front Environ Sci 10:941490
Hu K, Zhang Q, Gong S et al. (2024) A review of anthropogenic ground-level carbon emissions based on satellite data. IEEE J Sel Top Appl Earth Observ Remote Sens
Hua Y, Zhao X, Sun W (2023) Estimation of anthropogenic CO_2 emissions at different scales for assessing SDG indicators: method and application. J Clean Prod 414:137547
Huang Q, Yang X, Gao B (2014) Application of DMSP/OLS nighttime light images: A meta-analysis and a systematic literature review. Remote Sens 6:6844–6866
Hughes S, Giest S, Tozer L (2020) Accountability and data-driven urban climate governance. Nat Clim Chang 10:1085–1090
Ialongo I, Bun R, Hakkarainen J (2023) Satellites capture socioeconomic disruptions during the 2022 full-scale war in Ukraine. Sci Rep 13:14954
IPCC (2006) Guidelines for national greenhouse gas inventories. Chapter I Introduction Prepared by the National Greenhouse Gas Inventories Programme
Jiang F, Chen B, Li P (2023) Spatio-temporal evolution and influencing factors of synergizing the reduction of pollution and carbon emissions-utilizing multi-source remote sensing data and GWTWR model. Environ Res 229:115775
Jiang W, He G, Long T (2017) Ongoing conflict makes Yemen dark: From the perspective of nighttime light. Remote Sens 9:798
Klein D (2017) The Paris Agreement on Climate Change: Analysis and Commentary. Oxford University Press
Lan T, Shao G, Tang L (2021) Quantifying spatiotemporal changes in human activities induced by the COVID-19 pandemic using daily nighttime light data. IEEE J Sel Top Appl Earth Observ Remote Sens 14:2740–2753
Lan X, Tans P, Thoning K (2025) Trends in globally-averaged CO_2 determined from NOAA global monitoring laboratory measurements. https://doi.org/10.15138/9N0H-ZH07
Leasure DR, Kashyap R, Rampazzo F (2023) Nowcasting daily population displacement in Ukraine through social media advertising data. Popul Dev Rev 49:231–254
Levin N, Ali S, Crandall D (2018) Utilizing remote sensing and big data to quantify conflict intensity: The arab spring as a case study. Appl Geogr 94:1–17
Li J, Jia K, Wei X (2022) High-spatiotemporal resolution mapping of spatiotemporally continuous atmospheric CO_2 concentrations over the global continent. Int J Appl Earth Obs Geoinf 108:102743
Li S, Cao X (2024) Monitoring the modes and phases of global human activity development over 30 years: Evidence from county-level nighttime light. Int J Appl Earth Obs Geoinf 126:103627
Li X, Li D (2014) Can night-time light images play a role in evaluating the Syrian crisis? Int J Remote Sens 35:6648–6661
Li X, Zhang R, Huang C (2015) Detecting 2014 Northern Iraq Insurgency Using Night-Time Light Imagery. Int J Remote Sens 36:3446–3458
Li X, Li D, Xu H et al. (2021) Intercalibration between DMSP/OLS and VIIRS night-time light images to evaluate city light dynamics of Syria's major human settlement during Syrian civil war. In: Remote Sensing of Night-Time Light. Routledge, p 80–97
Li Z, Ouyang X, Du K (2017) Does government transparency contribute to improved eco-efficiency performance? An empirical study of 262 cities in China. Energy Policy 110:79–89
Liu X, Ou J, Wang S (2018) Estimating spatiotemporal variations of city-level energy-related co2 emissions: An improved disaggregating model based on vegetation adjusted nighttime light data. J Clean Prod 177:101–114
Liu Y, Xie X, Wang M (2023a) Energy structure and carbon emission: Analysis against the background of the current energy crisis in the eu. Energy 280:128129
Liu Z, Ciais P, Deng Z (2020a) Carbon monitor, a near-real-time daily dataset of global CO_2 emission from fossil fuel and cement production. Sci Data 7:392
Liu Z, Qiu Q, Li J (2020b) Geographic optimal transport for heterogeneous data: Fusing remote sensing and social media. IEEE Trans Geosci Remote Sens 59:6935–6945
Liu Z, Deng Z, Zhu B (2022) Global patterns of daily CO_2 emissions reductions in the first year of COVID-19. Nat Geosci 15:615–620
Liu Z, Deng Z, Huang X (2023b) A carbon-monitoring strategy through near-real–time data and space technology. Innovation 4(1)
Liu Z, Li J, Chen H (2024a) Prediction of changes in war-induced population and CO_2 emissions in Ukraine using social media. Hum Soc Sci Commun 11:1–11
Liu Z, Li J, Wang L et al. (2024b) Optimal transport under land cover information constraints: Fusing heterogeneous sar imagery and social media data. IEEE Trans Geosci Remote Sens
Mees H, Driessen P (2019) A framework for assessing the accountability of local governance arrangements for adaptation to climate change. J Environ Plan Manag 62:671–691
Morar C, Lukić T, Valjarević A (2022) Spatiotemporal analysis of urban green areas using change detection: A case study of Kharkiv, Ukraine. Front Environ Sci 10:823129
Mortoja MG, Yigitcanlar T (2022) Understanding political bias in climate change belief: A public perception study from south east queensland. Land Use Pol 122:106350
Mu T, Zheng Q, He SY (2024) Robust disaster impact assessment with synthetic control modeling framework and daily nighttime light time series images. IEEE Trans Geosci Remote Sensing
Mubarik MS, Kashif M, Shabbir M (2024) Sustainable management in natural resources and carbon neutrality: Revisiting the nexus in Ukraine-Russia war context. Resour Policy 97:105279
Oda T, Maksyutov S, Andres RJ (2018) The open-source data inventory for anthropogenic CO_2, version 2016 (odiac2016): a global monthly fossil fuel CO_2 gridded emissions data product for tracer transport simulations and surface flux inversions. Earth Syst Sci Data 10:87–107
Pan G, Xu Y, Ma J (2021) The potential of CO_2 satellite monitoring for climate governance: A review. J Environ Manage 277:111423
Pandey B, Zhang Q, Seto KC (2017) Comparative evaluation of relative calibration methods for DMSP/OLS nighttime lights. Remote Sens Environ 195:67–78
Piao S, Friedlingstein P, Ciais P et al. (2007) Growing season extension and its impact on terrestrial carbon cycle in the northern hemisphere over the past 2 decades. Glob Biogeochem Cycle 21(3)
Qi D, Majda AJ (2020) Using machine learning to predict extreme events in complex systems. Proc Natl Acad Sci 117:52–59
Rahman MM, Kashem MA (2017) Carbon emissions, energy consumption and industrial growth in Bangladesh: Empirical evidence from ARDL cointegration and Granger causality analysis. Energy Policy 110:600–608
Raleigh C, Linke R, Hegre H (2010) Introducing ACLED: An armed conflict location and event dataset. J Peace Res 47:651–660

Ratnayake R, Abdelmagid N, Dooley C (2022) What we do know (and could know) about estimating population sizes of internally displaced people. J Migration Health 6:100120
Rawtani D, Gupta G, Khatri N (2022) Environmental damages due to war in Ukraine: A perspective. Sci Total Environ 850:157932
Redmond L, Convery F (2015) The global carbon market-mechanism landscape: pre and post 2020 perspectives. Clim Policy 15:647–669
Román MO, Wang Z, Sun Q (2018) Nasa's black marble nighttime lights product suite. Remote Sens Environ 210:113–143
Sasmoko IM, Khan S (2023) War psychology: The global carbon emissions impact of the Ukraine-Russia conflict. Front Environ Sci 11:1065301
Schneider L, La Hoz Theuer S (2019) Environmental integrity of international carbon market mechanisms under the Paris agreement. Clim Policy 19:386–400
Shi K, Yu B, Zhou Y (2019) Spatiotemporal variations of CO_2 emissions and their impact factors in China: A comparative analysis between the provincial and prefectural levels. Appl Energy 233:170–181
Shi K, Shen J, Wu Y (2021) Carbon dioxide (CO_2) emissions from the service industry, traffic, and secondary industry as revealed by the remotely sensed nighttime light data. Int J Digit Earth 14:1514–1527
Söder R (2023) Climate change, security and military organizations: Changing notions in the Swedish armed forces. Earth Syst Gov 15:100169
Sun J, Qi Y, Guo J (2024) Impact of nighttime light data saturation correction on the application of carbon emissions spatialization: A comparative study of the correction effect and application effect based on five methods in China. J Clean Prod 438:140815
Telesetsky A (1999) The Kyoto Protocol. Ecol Law Quart 26:797–813
Tian, W, Zhang L, Yu T et al. (2024) Using multi-source data and time series features to construct a global terrestrial CO_2 coverage by deep learning. IEEE Trans Geosci Remote Sensing
Valjarević A, Milanović M, Gultepe I (2022) Updated Trewartha climate classification with four climate change scenarios. Geogr J 188:506–517
Wang S, Cheng C, Chen S (2024) Development of china's atmospheric environment monitoring satellite co2 ipda lidar retrieval algorithm based on airborne campaigns. Remote Sens Environ 315:114473
Wang Z, Román MO, Kalb VL (2021) Quantifying uncertainties in nighttime light retrievals from suomi-npp and noaa-20 viirs day/night band data. Remote Sens Environ 263:112557
Williams E (2020) Attributing blame?–Climate accountability and the uneven landscape of impacts, emissions, and finances. Clim Change 161:273–290
Wilmot TY, Lin JC, Wu D (2024) Toward a satellite-based monitoring system for urban CO_2 emissions in support of global collective climate mitigation actions. Environ Res Lett 19:084029
Xu JH, Wang, X Su, J et al (2025) Assessing the coordination and consistency of china's carbon peak and carbon neutrality policy system based on text and network analysis methods. Available at SSRN 5101531
Yu B, Liu J, Lyu T (2022) A new detection method to assess the influence of human activities and climate change of CO_2 emissions in coal fields. Ecol Indic 143:109417
Zheng Q, Seto KC, Zhou Y (2023) Nighttime light remote sensing for urban applications: Progress, challenges, and prospects. ISPRS J Photogramm Remote Sens 202:125–141
Zou S, Fan X, Wang L (2024) High-speed rail new towns and their impacts on urban sustainable development: a spatial analysis based on satellite remote sensing data. Humanities and Social Sciences Communications 11:1–13

Acknowledgements
This work was supported by the National Natural Science Foundation of China under Grant 62401526 and Grant T2225019.

Author contributions
Conceptualization: ZL, JL, and HC. Formal analysis: ZL and JL Software: ZL and HC. Supervision: JL, LW, and AP. Visualization: ZL. Writing: ZL.

Competing interests
The authors declare no competing interests.

Ethical approval
This study did not involve any experiments with human participants or animals performed by any of the authors.

Informed consent
This study did not involve human participants, and thus, no informed consent was required.

Additional information
Supplementary information The online version contains supplementary material available at https://doi.org/10.1057/s41599-025-05151-w.

Correspondence and requests for materials should be addressed to Zhenjie Liu, Jun Li, Haonan Chen, Lizhe Wang or Antonio Plaza.